

An investigation of effect of mass flow rate variation on productivity, exergoeconomic and enviroeconomic parameters of N similar PVTCPs included with double slope solar still

Desh Bandhu Singh^{a,*}, Devesh Kumar^b, Rakesh Kumar Yadav^c, Sanjeev Kumar Sharma^d, Yatender Chaturbedi^e, Navneet Kumar^f, Vijay Kumar Dwivedi^b

^aDepartment of Mechanical Engineering, Graphic Era Deemed to be University, Bell Road, Clement Town, Dehradun – 201306, Uttarakhand, India, email: dbsit76@gmail.com/deshbandhusingh.me@geu.ac.in

^bMadan Mohan Malviya University of Technology, Gorakhpur, Uttar Pradesh, 273010, India, emails: dkme@mmmut.ac.in (D. Kumar), vkdwivedi94@gmail.com (V.K. Dwivedi)

^cShri Venkateshwara University, NH-24, Gajraula, Amroha – 244236, U.P., India, email: er.rakeshyadava@gmail.com

^dDepartment of Mechanical Engineering, Amity School of Engineering and Technology, Noida, Uttar Pradesh 201301, India, email: sksharma.me@gmail.com

^eDepartment of Electrical and Electronics Engineering, Sunderdeep Group of Institutions, Ghaziabad, email: yatender.neeru@gmail.com

^fGalgotias College of Engineering and Technology, Greater Noida – 201306, G.B. Nagar, Uttar Pradesh, India, email: navneet.kumar@galgotiacollege.edu

Received 16 May 2021; Accepted 24 September 2021

ABSTRACT

This research paper deals with an investigation of effect of mass flow rate (\dot{m}_f) variation on productivity, exergoeconomic and enviroeconomic parameters of N similar PVT compound parabolic concentrators included with double slope solar still keeping water depth as 0.14 m. All the four types of weather situation for the climatic condition of New Delhi have been considered for the estimation of parameters. All relevant data and equations have been made input to computational programme written in MATLAB-2015a for getting values of parameters for different values of \dot{m}_f , keeping N constant to know the effect of dissimilarity of \dot{m}_f on productivity, exergoeconomic and enviroeconomic parameters for double slope active solar still. It has been concluded that the values of productivity and enviroeconomic parameters diminish with the enhancement in the value of \dot{m}_f at given value of water depth of 0.14 m till $\dot{m}_f = 0.11$ kg/s and then become almost constant.

Keywords: Exergoeconomic; Enviroeconomic; Productivity; Mass flow rate; Active solar still

1. Introduction

The fresh water is one of the basic needs for the life to survive on earth. However, fresh water is not available in abundance to meet the need of human beings as there is scarcity of fresh water throughout the world.

The purification of water by conventional method needs electrical energy and the generation of electrical energy emits polluting elements that pollutes the surrounding. Hence, conventional energy source is not beneficial for the environment because of the of greenhouse gases emission. The solar energy technology-based systems which

* Corresponding author.

are simple and environment friendly has the potential to meet both energy as well as freshwater needs. The double slope active solar still involving solar panel can generate direct current (DC) electric power as well as fresh water. This type of solar energy-based system is self-sustainable and hence can be installed and operated successfully at the remote locations where sunlight is present in abundance. The productivity analysis of the solar energy-based system is essential because it tells whether the system is technically feasible from energy and exergy viewpoints. If the value of productivity is more than 100%, the system is feasible.

The solar energy operated water purifier (SEOWP) in active mode was reported in 1983 [1] for the first time and from that time, many new designs have been reported by various researchers around the globe. The active type SEOWP means the provision of external source of heat to the basin of passive type SEOWP. The external source of heat can be made available as solar collectors/industry waste heat using heat exchanger or similar other kinds of provision can be made. Rai and Tiwari [1] reported the enhancement in yield of active type SEOWP by incorporating one conventional flat plate collector (FPC) over passive type SEOWP of the same basin area due to the supply of heat to the basin in active mode of operation. This water purifier was not self-sustainable as the pump needed some electric power for working which was supplied through grid.

The active type SEOWP in the forced mode of operation can be made self-sustainable by incorporating solar panel. Kumar and Tiwari [2] proposed the integration of PVT with FPC for supplying heat to basin of passive type SEOWP taking inspiration from the work of Kern and Russell [3]. It was reported by Kern and Russell that the electrical efficiency of solar panel got increased upon integration of solar panel with solar collector due to the removal of heat by fluid passing below the panel. Kumar and Tiwari reported the improvement in output by 3.5 times over the similar passive type SEOWP due to the addition of heat by two collectors in which only one of them was integrated with PVT for making the system self-sustainable. The work of Kumar and Tiwari was extended by Singh et al. [4] for double slope (DS) type SEOWP in active mode. Further, Singh et al. [5] and Tiwari et al. [6] reported the experimental investigation of SEOWP by incorporating two FPCs in which both FPCs were partially integrated with PVT. They reported an enhancement in DC electrical output; however, the yield of fresh water was less as compared to the system reported by Kumar and Tiwari [2]. It happened since heat gain was less because more area of FPCs were covered by PVT. Further, active type SEOWP was studied under optimized situation [7–11]. It was reported that the DS type SEOWP under optimized condition by incorporating N alike PVT-FPCs had 74.66% higher energy payback time (ENPBT) over passive type DS-SEOWP. The value of exergoeconomic parameter for single slope type SEOWP was found to be 47.37% higher than the passive type single slope SEOWP of same basin area. Sahota and Tiwari [12] reported the use of nanofluid in DS type SEOWP in active mode for enhancing the fresh water output. Carranza et al. [13] have experimentally investigated the performance of DS type SEOWP loaded with nanofluid by incorporating preheating of saline water and

concluded that water yield increases due to better thermophysical properties of nanofluid as compared to base fluid. Kouadri et al. [14] have investigated solar still by incorporating zinc and copper oxides for the location of Algeria and compared the yield with conventional SEOWP and concluded that the water yield was improved by 79.39% due to having better thermophysical characteristic of nanofluid.

The output of SEOWP could further be enhanced by changing the design of solar collector which could absorb higher amount of heat from the sun or by changing the design of solar still. PVT integrated FPC could gain higher heat if some concentrating part was integrated with FPC. With this concept in mind, Atheaya et al. [15] proposed PVT integrated compound parabolic concentrator collector (CPC) and reported its thermal model which was further extended by Tripathi et al. [16] for N collectors connected in series and loop was opened. Singh and Tiwari [17–19], Gupta et al. [20,21], Singh et al. [22,23] and Sharma et al. [24] investigated SEOWP of basin type by incorporating characteristic equations development and concluded that SEOWP of double slope type performs better than SEOWP of single slope type under optimized conditions of mass flow rate and number of collectors at 0.14 m water depth due to better distribution of solar energy in the case of double slope type. Prasad et al. [25], Bharti et al. [26], Singh [27] investigated SEOWP of double slope type from sensitivity viewpoint and concluded that the sensitivity analysis helps designer and installer of solar systems as which parameter should be focused more for a particular application.

The heat gain by solar collector can be enhanced by providing evacuated tubes because convection loss does not take place through vacuum. Sampathkumar et al. [28] investigated the SEOWP by incorporating evacuated tubular collector and reported an increase of 129% over the SEOWP of the same basin area due to the addition of heat to the basin by collectors. An investigation of SEOWP in natural mode of operation by incorporating evacuated tubes was done by Singh et al. [29] and reported exergy efficiency lying in the range of 0.15–8%. Further, an investigation of SEOWP incorporated with evacuated tubes was done in forced mode of operation by inserting pump between collector and basin and reported enhanced fresh water output as compared to the similar system operated in natural mode due to better circulation of fluid in the forced mode of operation [30]. Mishra et al. [31] reported characteristic equation development for N alike series connected ETCs. The work reported by Mishra et al. [31] was further extended by Singh et al. [32–34]. The thermal modeling of basin type SEOWP by incorporating N alike ETCs was reported by them, and comparison was also made between single slope active water purifier and DS type SEOWP in active mode taking energy, exergy, energy metrics, exergoeconomic and enviroeconomic parameters as basis. Issa and Chang [35] further extended the work of Singh et al. by connecting ETCs in mixed mode of operation experimentally and reported enhanced output as compared to similar set up in passive mode due to heat addition by collectors in active mode. Moreover, Singh and Al-Helal [36], Singh et al. [37] and Sharma et al. [38,39] reported development of characteristic equations and the observations based on the energy metrics for SEOWP by incorporating evacuated tubular collector as

well as compound parabolic concentrator integrated evacuated tubular collector.

Patel et al. [40–42] have reviewed SEOWP recently by incorporating different types of collectors. Further, Singh et al. [43] reviewed SEOWP by incorporating different types of collectors and loaded with nanofluid with an aim to find the effect of nanofluid on the performance of active SEOWP. Nanofluid is obtained by mixing a small amount of nanoparticles to water. The effect of adding nanoparticles to water in SEOWP is to increase the output (potable water and exergy) of SEOWP. The better performance of nanofluid loaded SEOWP than loaded with water is due to the possession of better thermo-physical characteristic of nanofluid as compared to water. Bansal et al. [44] have reported the mini review of changing the material of absorber on the performance of solar still. Shankar et al. [45] have studied ETC integrated SEOWP in natural as well forced mode and concluded that forced mode is better for environment as higher carbon credit was observed in forced mode due to more addition of heat to basin in the case of forced mode. Abdallah et al. [46] have investigated spherical and pyramid basin SEOWP and concluded that the spherical basin SEOWP gave 57.1% higher water yield due to better utilization of solar radiation in the case of spherical basin.

From the current literature survey, it is seen that the effect of mass flow rate (\dot{m}_f) on the annual productivity, exergoeconomic and enviroeconomic parameters of DS type SEOWP by incorporating N alike PVTCPs has not been reported by any researcher. The difference between the earlier reported work and the proposed work lies in the fact that the annual productivity, exergoeconomic and enviroeconomic parameters active type SEOWP was computed at a fixed value of \dot{m}_f ; whereas, in the proposed work, the annual productivity, exergoeconomic and enviroeconomic parameters

of DS type SEOWP in active mode has been estimated by varying values of \dot{m}_f on the performance parameters.

2. System metaphors

The DS type SEOWP by incorporating N alike partly covered PVTCPs having series connection has been shown in Fig. 1 and its specification in Table 1. In the proposed SEOWP, heat is provided by N equal partially covered PVTCPs and hence works in active mode. When sunlight falls on the surface of condensing cover, it is transmitted to water surface after reflection and absorption. The transmittivity of the glass is about 0.95. So, major portion of sunlight is transmitted to water surface. Again, after reflection and absorption by water surface, the sunlight is transmitted to blackened surface kept at the bottom of basin where almost all parts of radiation gets absorbed. The temperature of blackened surface kept at the bottom rises and heat is transferred to water from the blackened surface. Water in the basin also receives heat from N alike series connected collectors. Thus, temperature of water rises, and evaporation occurs which depends on the temperature difference between water surface and inside surface of glass cover. The vapor gets condensed through film wise condensation at the inside surface of glass. The condensed water trickles down under the gravity and gets collected at the channel fixed at the lower side. The fresh water is then collected in jar through tube connected to the channel.

3. Mathematical modeling based on energy balance equations

Mathematical modeling of N equal partially covered PVTCPs integrated to DS type SEOWP means writing

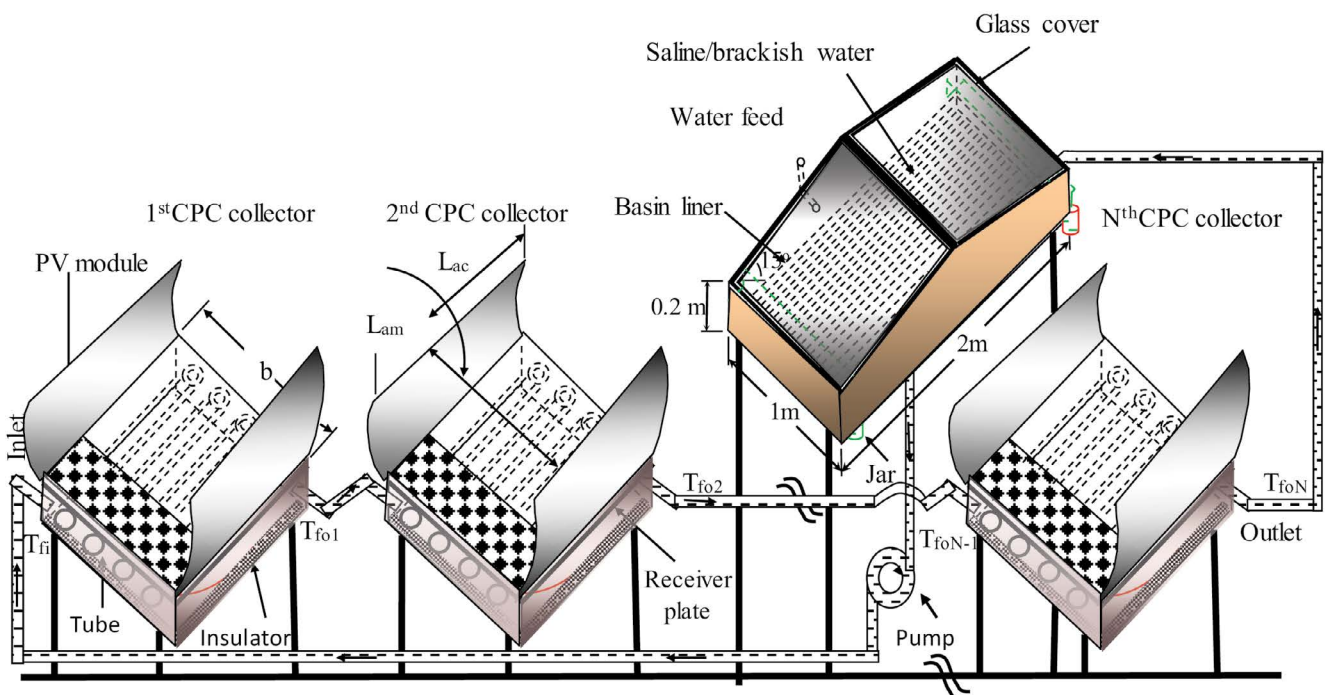


Fig. 1. Schematic diagram of DS type SEOWP integrated with N equal partially covered PVTCPs having series connection [17].

equations for all its components by equating input energy to output energy. Following assumptions presented in Singh and Tiwari [19], the mathematical modeling can be done as follows:

3.1. The heat gain for N equal partially covered PVTCPs

The heat gain from N equal partially covered PVTCPs and temperature at the outlet of last collector can be written as follows [13,14]:

$$\dot{Q}_{uN} = \frac{(1-K_k^N)}{(1-K_k)} (AF_R(\alpha\tau))_1 I_b(t) + \frac{(1-K_k^N)}{(1-K_k)} (AF_R U_L)_1 (T_{fi} - T_a) \quad (1)$$

$$T_{ioN} = \frac{I_b(t)(AF_R(\alpha\tau))_1 (1-K_k^N)}{\dot{m}_f C_f (1-K_k)} + \frac{(T_a (AF_R U_L))_1 (1-K_k^N)}{\dot{m}_f C_f (1-K_k)} + T_{fi} K_k^N \quad (2)$$

Here, $T_{fi} = T_w$. NPVTCPs are in closed loop in the proposed water purifier as the fluid at the outlet of last collector is allowed to flow to the basin of solar still. Hence, $T_{wo} = T_{ioN}$.

The electrical efficiency of solar cells (η_{cN}) of NPVTCPs can be expressed as [47,48]

$$\eta_{cN} = \eta_o [1 - \beta_o (\bar{T}_{cN} - T_o)] \quad (3)$$

Here, η_o stands for efficiency under standard state test condition and \bar{T}_{cN} stands for average value of temperature of solar cell of NPVTCPs.

3.2. Mathematical equation based on equating input and output energies for DS type SEOWP in active mode

The fundamental equations for different components of DS type SEOWP in active mode taking balancing energy as basis can be written as follows:

3.2.1. For inside surface of glass cover facing east

$$\begin{aligned} \alpha'_g I_{SE}(t) A_{gE} + h_{1wE} (T_w - T_{giE}) \frac{A_b}{2} - h_{EW} (T_{giE} - T_{giW}) A_{gE} \\ = \frac{K_g}{L_g} (T_{giE} - T_{goE}) A_{gE} \end{aligned} \quad (4)$$

where $h_{1wE} = h_{rwgE} + h_{cwgE} + h_{ewgE}$ which is called net heat transfer coefficient (NHTC) from surface of water to inside surface of glass cover and α'_g represents the fraction of solar flux absorbed by the glass cover.

3.2.2. For outside surface of glass cover facing east

$$\frac{K_g}{L_g} (T_{giE} - T_{goE}) A_{gE} = h_{1gE} (T_{goE} - T_a) A_{gE} \quad (5)$$

where $h_{1gE} = h_{rgE} + h_{cgE}$ or $h_{1gE} = 5.7 + 3.8$ V

3.2.3. For inside surface of glass cover facing west

$$\begin{aligned} \alpha'_g I_{SW}(t) A_{gW} + h_{1wW} (T_w - T_{giW}) \frac{A_b}{2} + h_{EW} (T_{giE} - T_{giW}) A_{gE} \\ = \frac{K_g}{L_g} (T_{giW} - T_{goW}) A_{gW} \end{aligned} \quad (6)$$

where $h_{1wW} = h_{rwgE} + h_{cwgE} + h_{ewgE}$ which is called NHTC from surface of water to inside surface of glass cover which is oriented towards east.

3.2.4. For outside surface of glass cover facing west

$$\frac{K_g}{L_g} (T_{giW} - T_{goW}) A_{gW} = h_{1gW} (T_{goW} - T_a) A_{gW} \quad (7)$$

where $h_{1gW} = h_{rgW} + h_{cgW}$ or $h_{1gW} = 5.7 + 3.8$ V

3.3.3. For blackened surface placed at the bottom of basin

$$\alpha'_b (I_{SE}(t) + I_{SW}(t)) \frac{A_b}{2} = h_{bw} (T_b - T_w) A_b + h_{ba} (T_b - T_a) A_b \quad (8)$$

where α'_b is the fraction of solar flux absorbed by basin liner.

3.3.4. For water mass in basin

$$\begin{aligned} (M_w C_w) \frac{dT_w}{dt} = (I_{SE}(t) + I_{SW}(t)) \alpha'_w \frac{A_b}{2} + h_{bw} (T_b - T_w) \\ A_b - h_{1w} (T_w - T_{giE}) \frac{A_b}{2} - h_{1w} (T_w - T_{giE}) \frac{A_b}{2} + \dot{Q}_{uN} \end{aligned} \quad (9)$$

On simplification of Eq. (1) and Eqs. (4)–(9) using mathematical concept and proper arrangement of various terms, one can obtain the expression for temperature of water as

$$T_w = \frac{\bar{f}_1(t)}{a_1} (1 - e^{-a_1 t}) + T_{w0} e^{-a_1 t} \quad (10)$$

After finding the value of T_w from Eq. (10), one can proceed to obtain glass temperature for NPVTCP integrated DS type SEOWP as follows.

$$T_{giE} = \frac{A_1 + A_2 T_w}{P} \quad (11)$$

$$T_{giW} = \frac{B_1 + B_2 T_w}{P} \quad (12)$$

$$T_{goE} = \frac{\frac{K_g}{L_g} T_{giE} + h_{1gE} T_a}{\frac{K_g}{L_g} + h_{1gE}} \quad (13)$$

$$T_{goW} = \frac{\frac{K_g T_{giW} + h_{1gW} T_a}{L_g}}{\frac{K_g}{L_g} + h_{1gW}} \quad (14)$$

The different unknown terms in Eqs. (1)–(14) are given in appendix-A. The fresh water output from NPVTCPC integrated DS type SEOWP can be written as:

$$\dot{m}_{ew} = \left[\frac{h_{ewE} \frac{A_b}{2} (T_w - T_{giE}) + h_{ewW} \frac{A_b}{2} (T_w - T_{giW})}{L} \right] \times 3600 \quad (15)$$

4. Analysis

For the analysis of the effect of \dot{m}_e and N on the productivity, exergoeconomic and enviroeconomic parameters of DS type SEOWP in active mode, 4 climatic situations for each month of year have been taken. These climatic situations can be defined by number of sunshine hours (N') and daily diffuse to daily global irradiation ratio (r') as follows:

- (a) Clear day (blue sky) $r' \leq 0.25$ and $N' \geq 9$ h
- (b) Hazy day (fully) $0.25 \leq r' \leq 0.50$ and $7 \text{ h} \leq N' \leq 9 \text{ h}$
- (c) Hazy and cloudy (partially) $0.50 \leq r' \leq 0.75$ and $5 \text{ h} \leq N' \leq 7 \text{ h}$
- (d) Cloudy day (fully) $r' \geq 0.75$ and $N' \leq 5$ h

4.1. Energy analysis

The expression of overall annual energy (E_{out}) for DS type SEOWP in active mode considering first law of thermodynamics can be expressed as:

$$E_{out} = \frac{(M_{ew} \times L)}{3600} + \frac{(P_m - P_u)}{0.38} \quad (16)$$

where M_{ew} is annual potable water output obtained from DS type SEOWP in active mode, P_m is yearly electrical power received from PVT, P_u is yearly electrical power utilized by pump and L is latent heat. Here, factor 0.38 which is present in the denominator converts electrical energy (high grade energy) into heat (a low grade energy). This factor is basically the efficacy of power output taken from conventional power plant [49].

The hourly electrical energy (\dot{E}_e) for the solar panel used in DS type SEOWP in active mode can be expressed as follows:

$$\dot{E}_e = A_m I_b(t) \sum_1^N (\alpha \tau_g \eta_{cN}) \quad (17)$$

Eq. (17) can be used for evaluating daily electrical exergy of type (a) climatic situation by summing the hourly value of 10 h because the solar flux exists for 10 h only. The similar approach has been used to work out the daily electrical

energy for rest types of climatic situation, that is, type (b) to type (d). The value of electrical energy on monthly basis for type (a) climatic situation has been evaluated as the multiplication of electrical energy on daily basis and the corresponding value of number of clear days (n'). The similar approach has been used to work out the electrical energy on monthly basis for rest types of climatic situation that is, type (b) to type (d). The value of net electrical energy on monthly basis has been worked out by summing electrical energies values for type (a) to type (d) climatic situations. The value of electrical energy (P_m) on annual basis has been worked out by the summing of electrical energy on monthly basis for 12 months. The similar approach has been followed for the evaluation of annual fresh water yielding (M_{ew}).

4.2. Exergy analysis

Exergy analysis has been done based on first law (energy) and second law (entropy) of thermodynamics. The hourly output thermal exergy $\dot{E}_{x,out}(W)$ for NPVTCPC integrated DS type SEOWP can be expressed as [50]

$$\begin{aligned} \dot{E}_{x,out} = & h_{ewgE} \times \frac{A_b}{2} \times \left[(T_w - T_{giE}) - (T_a + 273) \times \ln \left\{ \frac{(T_w + 273)}{T_{giE} + 273} \right\} \right] \\ & + h_{ewgW} \times \frac{A_b}{2} \times \left[(T_w - T_{giW}) - (T_a + 273) \times \ln \left\{ \frac{(T_w + 273)}{T_{giW} + 273} \right\} \right] \end{aligned} \quad (18)$$

where

$$h_{e,wg} = 16.273 \times 10^{-3} h_{c,wg} \left[\frac{P_w - P_{gi}}{T_w - T_{gi}} \right] \quad [51] \quad (19)$$

$$h_{c,wg} = 0.884 \left[(T_w - T_{gi}) + \frac{(P_w - P_{gi})(T_w + 273)}{268.9 \times 10^3 - P_w} \right]^{1/3} \quad [52] \quad (20)$$

$$P_w = \exp \left[25.317 - \frac{5144}{(T_w + 273)} \right] \quad (21)$$

and

$$P_{gi} = \exp \left[25.317 - \frac{5144}{(T_{gi} + 273)} \right] \quad (22)$$

Eq. (18) can be used for evaluating daily thermal exergy of type (a) climatic situation by summing the hourly value of 10 h because the solar flux exists for 10 h only. The similar approach has been used to work out the daily thermal exergy for rest types of climatic situation, that is, type (b) to type (d). The value of thermal exergy on monthly basis for type (a) climatic situation has been evaluated as the multiplication of thermal exergy on daily basis and the corresponding value of number of clear days (n'). The similar approach has been used to work out the thermal exergy on monthly

basis for rest types of climatic situation, that is, type (b) to type (d). The value of net thermal exergy on monthly basis has been worked out by summing thermal exergies values for type (a) to type (d) climatic situations. The value of thermal exergy on annual basis has been worked out by the summing of thermal exergy on monthly basis for 12 months.

The value of yearly overall annual exergy gain ($G_{ex,annual}$) for DS type SEOWP in active mode has been expressed as follows:

$$G_{ex,annual} = Ex_{out} + (P_m - P_u) \quad (23)$$

4.3. Exergoeconomic analysis

The value of exergoeconomic parameter has been estimated using first and second laws of thermodynamics. This relationship means that the system is constructed in such a way that it achieves an overall optimum design by efficiently balancing the exergy and economic parameters. The exergoeconomic parameter relates either exergy loss or exergy gain with uniform end of year annual cost (UEOYAC). In the case of exergy gain, the objective is maximization type, whereas, in the case of exergy loss, the objective is minimization type. The exergoeconomic parameter can be estimated as:

$$\text{Exergoeconomic parameter} = \frac{\text{Annual exergy gain for SEOWP integrated with NPVTCPs} (G_{ex,annual})}{\text{UEOYAC}} \quad (24)$$

The value of annual exergy gain for SEOWP of double slope type integrated with N similar PVTCPs can be estimated using Eq. (23). The value of UEOYAC for SEOWP of double slope type integrated with N alike PVTCPs can be estimated as [53]:

$$\text{UEOYAC} = PC \times CRF + MC \times CRF - SV \times SFF \quad (25)$$

where PC, SV, CRF, SFF and MC stand for present cost, salvage value, capital recovery factor, sinking fund factor and maintenance cost in that order. The value of MC may be estimated as the multiplication of PC with maintenance cost factor that is normally considered as 0.1. The value of CRF which is used for converting PC into UEOYAC and can be expressed as:

$$CRF = \frac{i \times (1+i)^n}{(1+i)^n - 1} \quad (26)$$

and SFF can be written as:

$$SFF = \frac{i}{(1+i)^n - 1} \quad (27)$$

SFF is applied for converting SV into UEOYAC. In this case, i and n stand for the rate of interest and system life, respectively.

The value of PC for a SEOWP of double slope type integrated with NPVTCPs with a 30-year life span can be calculated as

$$PC = PI + P_u + \frac{P_u}{(1+i)^{10}} + \frac{P_u}{(1+i)^{20}} \quad (28)$$

where

$$PI = \text{Cost of solar still} + \text{Cost of PVTCPs} + \text{Fabrication cost} \quad (29)$$

The cost of fabrication also involves piping and labor. Values of UEOYAC have been evaluated using Eq. (25).

4.4. Enviroeconomic analysis

It provides economic incentive for controlling environmental pollution so that the emission of pollutants can be reduced and motivates individual to apply renewable energy technology which does not affect the environment. It can be estimated as:

$$\left(\text{Enviroeconomic parameter} \right)_{\text{energy}} = \left(\frac{(\text{Annual energy out}) \times (0.002)(CRP)}{n - \text{Embodied energy}} \right) \quad (30)$$

$$\left(\text{Enviroeconomic parameter} \right)_{\text{exergy}} = \left(\frac{(\text{Annual exergy out}) \times (0.002)(CRP)}{n - \text{Embodied energy}} \right) \quad (31)$$

CRP stands for carbon dioxide reduction price which can be taken as \$14.5.

4.5. Productivity

Productivity gives the relation between output and input and it is different from efficiency in the sense that the value of productivity should always be more than 100% whereas the value of efficiency should be less than 100%. Higher the productivity better will be the living standard of persons because higher productivity means more products are available for use. It is also expressed as the ratio of effectiveness and efficiency. The value of annual productivity for SEOWP of double slope type integrated with PVTCPs can be estimated as [54–57]:

$$\text{Productivity} = \frac{\text{Output from SEOWP integrated with NPVTCPs}}{\text{Input provided to SEOWP integrated with NPVTCPs}} \times 100 \quad (32)$$

Here, output from SEOWP of single slope type integrated with ETCs represents the annual fresh water produced from the system. This output can be expressed in terms of rupees by multiplying the amount of annual fresh

water in kg with unit cost (Rs./kg) of fresh water sold in the market. Hence, output from SEOWP of DS type integrated with NPVTCPs in terms of Rs. can be written as

$$\begin{aligned} \text{Output from DS type SEOWP integrated with PVTCPs} \\ = [(\text{Annual yield}) \times (\text{Selling price of water})] + \\ [(\text{Annual electric output}) \times (\text{Selling price of electricity})] \end{aligned} \quad (33)$$

Input provided to SEOWP of double slope type integrated with N similar PVTCPs will be UEOYAC and it can be estimated using Eq. (31). The productivity has been evaluated using Eq. (26) and has been presented in Table 5.

5. Methodology

The methodology to investigate the effect of \dot{m}_f and N on productivity, exergoeconomic and enviroeconomic parameters of DS type SEOWP integrated with N equal partially covered PVTCPs in forced mode are as follows:

- *Step I:* Taking the value of solar flux on the horizontal plane from IMD located at Pune in India, the value of solar flux on inclined plane has been evaluated using Liu and Jordan formula [58] by computational program in MATLAB. The data for surrounding temperature has been accessed from IMD situated at Pune in India.

- *Step II:* The computation for potable water yielding per hour basis for different values of \dot{m}_f at given N has been carried out with the help of Eq. (15) followed by the computation of potable water yielding on per year basis.
- *Step III:* The calculation for gross energy output values at various values of \dot{m}_f for given N have been performed using Eq. (16) followed by calculation for gross energy output on per year basis.
- *Step IV:* The computation for exergy on the basis of per hour for different values of \dot{m}_f at given N has been carried out with the help of Eqs. (17) and (18) followed by the calculation for exergy on per year basis. Further, gross exergy has been evaluated using Eq. (23).
- *Step V:* The exergoeconomic parameter, enviroeconomic parameter on the basis of energy as well as exergy and productivity have been estimated using Eqs. (24), (30), (31) and (32) in that order.

The flow chart for better understanding of methodology followed for the estimation of dissimilarity of mass flow rate on the performance of DS type SEOWP by incorporating N alike PVTCPs has been revealed as Fig. 2.

6. Results and discussion

The required data and all relevant equations have been fed to computational program written in MATLAB. Data on the horizontal surface has been taken from IMD Pune India.

Table 1
Specifications of DS type SEOWP integrated with N equal partially covered PVTCPs

Component	Specification	Component	Specification
Double slope active solar still			
Length	2 m	Orientation	East-west
Width	1 m	Thickness of glass cover	0.004 m
Inclination of glass cover	15°	K_g	0.816 W/m-K
Height of smaller side	0.2 m	Thickness of insulation	0.1 m
Material of body	GRP	Thermal conductivity of insulation	0.166 W/m-K
Material of stand	GI		
Cover material	Glass		
PVT-CPC collector			
Type and no. of collectors	Tube in plate type, N	Aperture area	2 m ²
Receiver area of solar water collector	1.0 m × 1.0 m	Aperture area of module	0.5 m × 2.0 m
Collector plate thickness	0.002	Aperture area of receiver	0.75 m × 2.0 m
Thickness of copper tubes	0.00056 m	Receiver area of module	0.25 m × 1.0 m
Length of each copper tubes	1.0 m	Receiver area of collector	0.75 m × 1.0 m
K_i (Wm ⁻¹ K ⁻¹)	0.166	F'	0.968
FF	0.8	ρ	0.84
Thickness of insulation	0.1 m	τ_g	0.95
Angle of CPC with Horizontal	30°	α_c	0.9
Thickness of toughen glass on CPC	0.004 m	β_c	0.89
Effective area of collector under glass	0.75 m ²	α_p	0.8
Pipe diameter	0.0125 m	Effective area of collector under PV module	0.25 m ²
DC motor rating	12 V, 24 W		

Data on the inclined surface has been evaluated using Liu and Jordan formula [58] with the help of MATLAB. The output of programme has been presented in Figs. 3–7 and Tables 2–7.

Table 2 represents the computation of yearly fresh water yield for NPVTCPC-SEOWP-DS at $\dot{m}_f = 0.02$ kg/s and $N = 4$. The water depth has been taken as 0.14 m. Similarly, fresh water yield at other values of \dot{m}_f has been evaluated and presented as Fig. 3. It is observed from Fig. 3 that the value of yield decreases as the value of \dot{m}_f increases. It happens because water flowing through tubes of collector gets less time to absorb heat at higher value of \dot{m}_f . The value of yield based on year decreases as the value of \dot{m}_f increases and then it becomes almost constant because after certain value of \dot{m}_f , heat absorbed by water is very small as water flowing through tubes does not get time to absorb heat from solar flux due to increased speed and the system behaves as working in passive mode.

Table 3 represents the computation of yearly thermal exergy for NPVTCPC-SEOWP-DS at $\dot{m}_f = 0.02$ kg/s and $N = 4$. The water depth has been taken as 0.14 m. Similarly, thermal exergy at other values of \dot{m}_f has been evaluated and presented as Fig. 4. It is observed from Fig. 4 that the value of thermal exergy decreases as the value of \dot{m}_f increases. It happens because water flowing through tubes of collector gets less time to absorb heat at higher value of \dot{m}_f , which result in less rise in temperature of water. The value of

thermal exergy based on year decreases as the value of \dot{m}_f increases and then it becomes almost constant because after certain value of \dot{m}_f , heat absorbed by water is very small as water flowing through tubes does not get time to absorb heat due to increased speed and the system behaves as working in passive mode.

Table 4 represents the computation of yearly electrical exergy for NPVTCPC-SEOWP-DS at $\dot{m}_f = 0.02$ kg/s and $N = 4$. The water depth has been taken as 0.14 m. Similarly, electrical exergy at other values of \dot{m}_f has been evaluated and presented as Fig. 5. It is observed from Fig. 5 that the value of electrical exergy increases as the value of \dot{m}_f increases. It happens because water flowing through tubes of collector takes away higher amount of heat from PVT at higher value of \dot{m}_f , which results in decrease in temperature of solar cell. Due to decreased temperature rise of solar cell, better efficiency is obtained and hence higher electrical exergy output. It is also observed that the value of electrical exergy output becomes almost constant after certain value of \dot{m}_f and then it becomes almost constant. It has been found to occur because water is not able to take away heat from PVT at very high velocity of water because water does not have time to consume water.

Figs. 6 and 7 represent the variation of yearly gross energy and yearly gross exergy respectively with different values of \dot{m}_f for NPVTCPC-SEOWP = DS at water depth of 0.14 m and $N = 4$. It is observed from Fig. 5 that the yearly gross energy

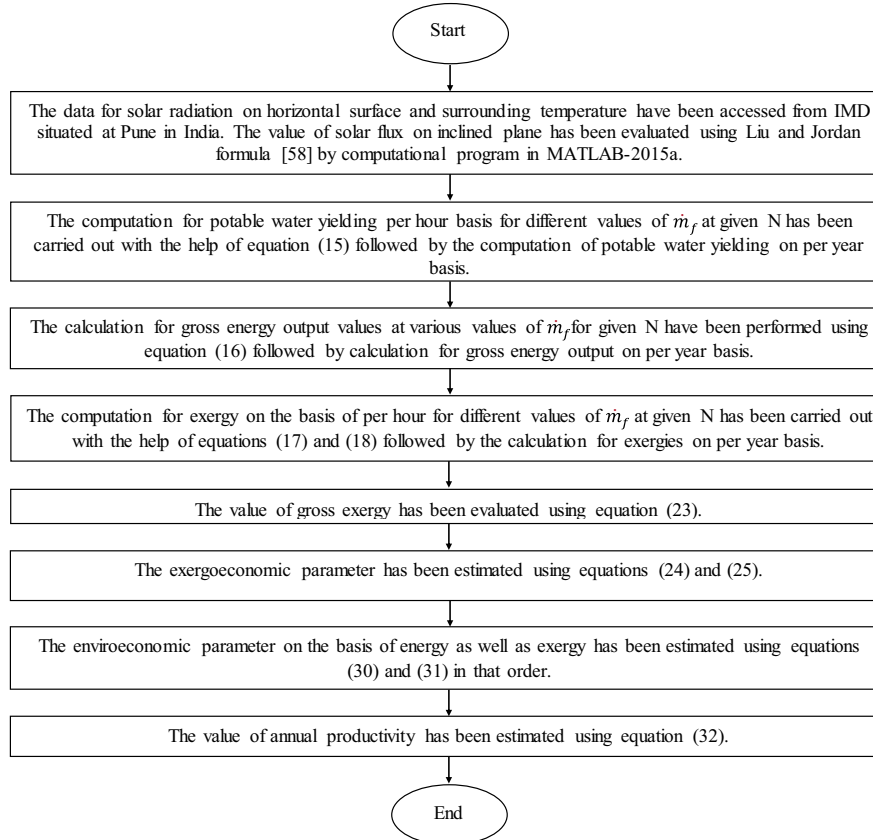


Fig. 2. Flow chart representing the methodology followed for the estimation of dissimilarity of mass flow rate on the performance of DS type SEOWP by incorporating N alike PVTCPs.

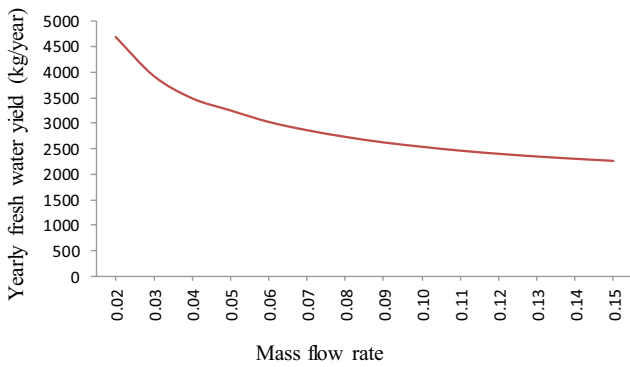


Fig. 3. Variation of yearly fresh water yield with \dot{m}_f for DS type SEOWP by incorporating N equal partially covered PVTCPs at $N = 4$.

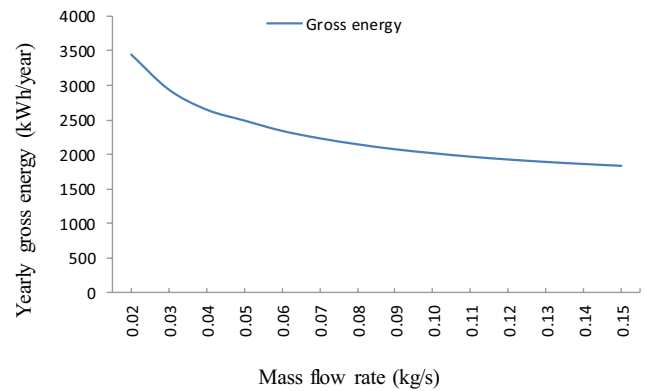


Fig. 6. Variation of yearly gross energy with \dot{m}_f for DS type SEOWP by incorporating N equal partially covered PVTCPs at $N = 4$.

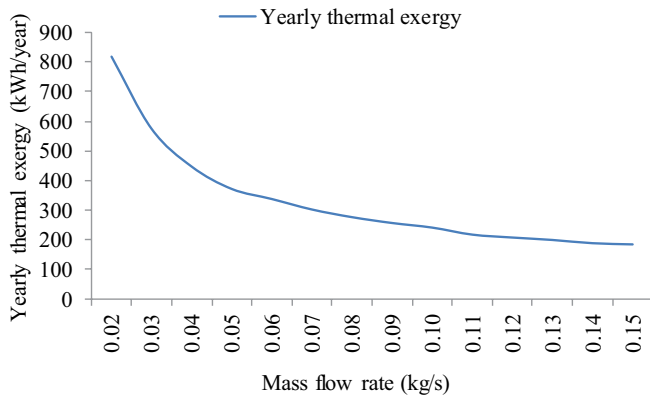


Fig. 4. Variation of yearly thermal exergy with \dot{m}_f for DS type SEOWP by incorporating N equal partially covered PVTCPs at $N = 4$.

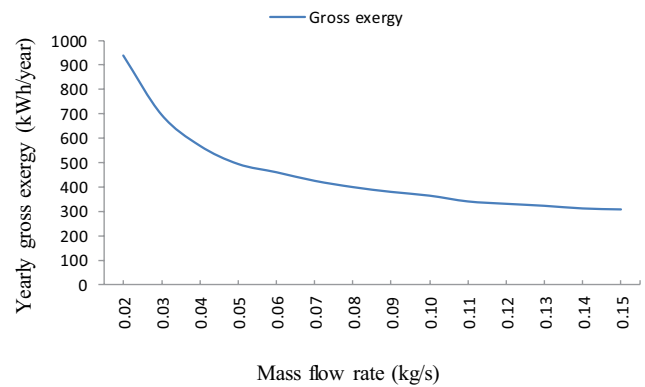


Fig. 7. Variation of yearly gross exergy with \dot{m}_f for DS type SEOWP by incorporating N equal partially covered PVTCPs at $N = 4$.

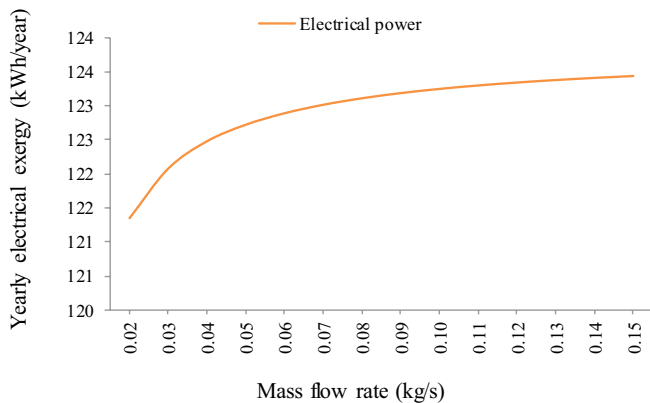


Fig. 5. Variation of yearly electrical exergy with \dot{m}_f for DS type SEOWP by incorporating N equal partially covered PVTCPs at $N = 4$.

decreases as the value of \dot{m}_f increases due to similar variation in yearly fresh water yield. It is observed from Eq. (16) that the value of gross energy output depends on energy output due water yielding and electrical exergy. The variation in energy and electrical exergy is opposite; however, decrease in energy output obtained due to water yielding overcomes the

increase in electrical exergy output with the increase in the value of \dot{m}_f . Hence, gross energy decreases with the increase in \dot{m}_f . It is observed from Fig. 7 that yearly gross exergy decreases as the value of \dot{m}_f increases. It happens because the variation in yearly thermal exergy and yearly electrical exergy is opposite; however, the decrease in yearly thermal exergy overcomes the increases in electrical energy/energy with the increase in value of \dot{m}_f .

Table 5 represents the capital investment for NPVTCP-SEOWP-DS based on the price of components in the local market and Table 6 presents the estimation of UEOYAC for NPVTCP-SEOWP-DS at $N = 4$ and water depth of 0.14 m. The interest rate has been considered as 2%, 5% and 10%. The interest depends on the policy of banking system. The life span of NPVTCP-SEOWP-DS has been considered as 30 year. The smallest value of UEOYAC has been obtained corresponding to 2% interest rate and 30 year life span. It has been so obtained because the interest rate of 2% is minimum. Table 7 represents the estimation of exergoeconomic parameter and enviroeconomic parameter for various values of \dot{m}_f for NPVTCP-SEOWP-DS at $N = 4$ and water depth of 0.14. Further, Fig. 8 represents the variation of exergoeconomic parameter graphically with \dot{m}_f considering different rate of interest for UEOYAC for DS type SEOWP by

Table 2
Computation of yearly fresh water yield for DS type SEOWP integrated with N equal partially covered PVTCPs at $m_j = 0.02 \text{ kg/s}$, $N = 4$ and water depth = 0.14 m

Monthly	Daily yield (Kind a)	Days (Kind a)	Monthly yield (Kind a)	Daily yield (Kind b)	Days (Kind b)	Monthly yield (Kind b)	Daily yield (Kind c)	Days (Kind c)	Monthly yield (Kind c)	Daily yield (Kind d)	Days (Kind d)	Monthly yield (Kind d)	Gross monthly yield
Jan.	24.27	3	72.82	28.13	8	225.02	6.80	11	74.77	1.57	9	14.11	386.73
Feb.	23.23	3	69.68	22.52	4	90.06	6.87	12	82.44	1.55	9	13.91	256.09
Mar.	25.74	5	128.69	26.65	6	159.88	11.48	12	137.76	5.57	8	44.58	470.91
April	27.79	4	111.16	27.68	7	193.79	11.64	14	162.97	9.54	5	47.72	515.64
May	27.09	4	108.36	20.72	9	186.50	13.98	12	167.75	7.95	6	47.70	510.31
June	37.02	3	111.06	20.93	4	83.72	12.24	14	171.42	4.25	6	25.48	391.67
July	22.67	2	45.34	17.63	3	52.90	12.13	10	121.26	3.56	17	60.58	280.08
Aug.	22.09	2	44.19	19.27	3	57.80	10.48	7	73.39	3.90	19	74.14	249.52
Sept.	29.23	7	204.61	25.71	3	77.14	14.24	10	142.39	5.39	10	53.87	478.02
Oct.	25.89	5	129.43	17.68	10	176.79	11.76	13	152.89	3.80	3	11.39	470.49
Nov.	23.34	6	140.01	14.75	10	147.53	5.25	12	63.00	4.30	2	8.60	359.15
Dec.	22.68	3	68.05	17.96	7	125.71	8.62	13	112.00	1.76	8	14.09	319.85
Yearly fresh water yield (kg)													4,688.47

Table 3
Computation of yearly thermal exergy for DS type SEOWP integrated with N equal partially covered PVTCPs at $m_j = 0.02 \text{ kg/s}$, $N = 4$ and water depth = 0.14 m

Daily exergy (kWh)	Days (Kind a)	Monthly exergy (Kind a) (kWh)	Daily exergy (Kind b)	Days (Kind b)	Monthly exergy (Kind b) (kWh)	Daily exergy (Kind c)	Days (Kind c)	Monthly exergy (Kind c) (kWh)	Daily exergy (Kind d)	Days (Kind d)	Monthly exergy (Kind d) (kWh)	Gross monthly exergy (kWh)
6.39	3	19.18	5.30	8	42.39	0.71	11	7.76	0.08	9	0.69	70.03
5.55	3	16.65	5.20	4	20.80	0.65	12	7.76	0.07	9	0.60	45.81
6.24	5	31.21	6.76	6	40.54	1.32	12	15.86	0.43	8	3.42	91.03
6.53	4	26.11	6.60	7	46.19	1.25	14	17.56	0.89	5	4.44	94.29
6.10	4	24.40	3.81	9	34.31	1.83	12	21.98	0.62	6	3.69	84.38
10.26	3	30.79	4.00	4	16.00	1.31	14	18.39	0.19	6	1.14	66.31
4.84	2	9.67	3.14	3	9.42	1.39	10	13.95	0.20	17	3.32	36.36
5.08	2	10.16	4.10	3	12.29	1.01	7	7.10	0.25	19	4.76	34.31
7.79	7	54.50	6.05	3	18.16	2.06	10	20.63	0.37	10	3.66	96.95
6.63	5	33.13	3.35	10	33.51	1.60	13	20.82	0.22	3	0.67	88.13
4.62	6	27.69	2.33	10	23.34	0.41	12	4.92	0.30	2	0.60	56.56
5.39	3	16.18	3.54	7	24.77	0.97	13	12.57	0.08	8	0.67	54.19
Yearly thermal exergy output (kWh)												818.35

Table 4
Computation of yearly electrical exergy for DS type SEOWP integrated with N equal partially covered PVTCPs at $\dot{m}_j = 0.02$ kg/s, $N = 4$ and water depth = 0.14 m

Daily exergy (kWh)	Days (Kind a)	Monthly exergy (Kind a) (kWh)	Daily exergy (kWh)	Days (Kind b)	Monthly exergy (Kind b) (kWh)	Daily exergy (kWh)	Days (Kind c)	Monthly exergy (Kind c) (kWh)	Daily exergy (kWh)	Days (Kind d)	Monthly exergy (Kind d) (kWh)	Gross monthly exergy (kWh)
0.646	3	1.939	0.596	8	4.769	0.309	11	3.397	0.124	9	1.114	11.219
0.616	3	1.849	0.600	4	2.401	0.299	12	3.588	0.108	9	0.968	8.807
0.597	5	2.984	0.609	6	3.652	0.339	12	4.069	0.210	8	1.677	12.381
0.566	4	2.264	0.567	7	3.967	0.301	14	4.215	0.256	5	1.279	11.724
0.523	4	2.092	0.432	9	3.890	0.317	12	3.801	0.195	6	1.173	10.956
0.670	3	2.010	0.456	4	1.825	0.284	14	3.976	0.139	6	0.833	8.644
0.495	2	0.990	0.415	3	1.244	0.302	10	3.020	0.122	17	2.077	7.331
0.510	2	1.020	0.461	3	1.382	0.262	7	1.833	0.142	19	2.689	6.924
0.561	7	3.927	0.512	3	1.536	0.337	10	3.373	0.155	10	1.547	10.383
0.552	5	2.760	0.443	10	4.435	0.342	13	4.452	0.145	3	0.434	12.081
0.546	6	3.277	0.396	10	3.959	0.211	12	2.534	0.184	2	0.368	10.138
0.588	3	1.763	0.516	7	3.611	0.337	13	4.376	0.127	8	1.013	10.763
Yearly electrical exergy output (kWh)												121.3501

Table 5
Capital investment for SEOWP of DS type incorporated with N similar PVT-CPCs for $N = 4$

S. No.	Parameter	Cost (₹)
1	Cost of solar still	19,183
2	Cost of N identical PVT collectors @10,500 each	42,000
3	Cost of motor and pump	1,000
4	Fabrication cost	6,000
5	Salvage value of the system after 30 years, if inflation remains @ 4% in India, [using present value of scrap material sold in Indian market]	21,790

Table 6
Estimation of UEYOAC for SEOWP of DS type incorporated with N similar partially covered PVTCPs at $N = 4$

n	i	P_s	M	S_s	$F_{CR,i,n}$	$F_{SR,i,n}$	UEYOAC
Yr.	%	₹	₹	₹	Fraction	Fraction	₹
30	2	69,676.32	6,967.63	21,790	0.03182	0.01182	2,181.253
30	5	69,173.80	6,917.38	21,790	0.05478	0.00478	4,064.119
30	10	68,717.19	6,871.72	21,790	0.10086	0.00086	7,605.158

incorporating N equal partially covered PVTCPs at $N = 4$. It has been observed from Table 7 and Fig. 8 that the value of exergoeconomic parameter decreases as the value of \dot{m}_j is increased till 0.11 kg/s and then becomes almost constant. It happens due to similar variation in gross exergy as the value of UEYOAC remains same. Similar variation has been observed in the value of enviroeconomic parameter. It has been observed that the value of exergoeconomic parameter decreases as the rate of interest is increased because increase in rate of interest increases the value of UEYOAC

and exergoeconomic parameter is inversely proportional to UEYOAC.

Table 8 presents the estimation of annual productivity for various values of \dot{m}_j for SEOWP of double slope type incorporated with N similar partially covered PVTCPs at $N = 4$ and water depth of 0.14. Further, Fig. 9 represents the variation of enviroeconomic parameter and annual productivity graphically with \dot{m}_j for DS type SEOWP by incorporating N equal partially covered PVTCPs at $N = 4$. It has been observed from Table 8 and Fig. 9 that

Table 7

Computation of exergoeconomic and enviroeconomic parameter for SEOWP of DS type incorporated with N similar partially covered PVTCPs at $N = 4$

Mass flow rate	Gross energy	Gross exergy	UEOYAC	Exergoeconomic parameter	Embodied energy	Enviroeconomic parameter (energy basis)	Enviroeconomic parameter (exergy basis)
kg/s	kWh	kWh	₹	₹	kWh	\$	\$
0.02	3,444.99	939.70	2,181.25	0.431	6,018.76	2,822.59	642.99
0.03	2,936.49	696.69	2,181.25	0.319	6,018.76	2,380.20	431.58
0.04	2,646.97	569.59	2,181.25	0.261	6,018.76	2,128.32	321.00
0.05	2,489.55	494.50	2,181.25	0.227	6,018.76	1,991.36	255.67
0.06	2,339.83	460.70	2,181.25	0.211	6,018.76	1,861.10	226.26
0.07	2,232.22	425.47	2,181.25	0.195	6,018.76	1,767.48	195.61
0.08	2,145.49	399.68	2,181.25	0.183	6,018.76	1,692.03	173.18
0.09	2,073.37	380.05	2,181.25	0.174	6,018.76	1,629.28	156.10
0.10	2,016.75	364.60	2,181.25	0.167	6,018.76	1,580.02	142.66
0.11	1,966.17	340.97	2,181.25	0.156	6,018.76	1,536.02	122.10
0.12	1,925.28	331.19	2,181.25	0.152	6,018.76	1,500.45	113.59
0.13	1,890.20	323.03	2,181.25	0.148	6,018.76	1,469.93	106.49
0.14	1,860.37	312.13	2,181.25	0.143	6,018.76	1,443.97	97.01
0.15	1,833.17	308.18	2,181.25	0.141	6,018.76	1,420.31	93.57

Table 8

Estimation of annual productivity for SEOWP of DS type incorporated with N similar partially covered PVTCPs at $N = 4$

Mass flow rate	Annual yield	Selling price of water	Annual electrical energy	Selling price of electricity	UEOYAC	Annual productivity
kg/s	kg	₹	kWh	kWh	₹	%
0.02	4,688.46	5	121.35	4	2,181.25	1096.97
0.03	3,922.84	5	122.08	4	2,181.25	921.60
0.04	3,486.98	5	122.48	4	2,181.25	821.76
0.05	3,249.89	5	122.72	4	2,181.25	767.46
0.06	3,024.64	5	122.89	4	2,181.25	715.86
0.07	2,862.74	5	123.02	4	2,181.25	678.77
0.08	2,732.27	5	123.11	4	2,181.25	648.89
0.09	2,623.78	5	123.19	4	2,181.25	624.03
0.10	2,538.61	5	123.25	4	2,181.25	604.51
0.11	2,462.54	5	123.30	4	2,181.25	587.09
0.12	2,401.03	5	123.34	4	2,181.25	572.99
0.13	2,348.27	5	123.38	4	2,181.25	560.91
0.14	2,303.40	5	123.41	4	2,181.25	550.63
0.15	2,262.50	5	123.44	4	2,181.25	541.26

the value of annual productivity decreases as the value of \dot{m}_f is increased. It happens because annual productivity depends on annual water yielding as well as annual electrical power output. The variation in annual water yielding and annual electrical power are opposite in nature; however, the decrease in revenue due to decrease in annual water yielding overcomes the increase in revenue due to increase in electrical power output which results in the decrease in annual productivity with the

increase in the value of \dot{m}_f . It is further observed that the value of annual productivity decreases at the fast rate till water depth of 0.11 m and then it becomes almost constant.

7. Conclusions

The analysis for NPVTCP-SEOWP-DS has been done considering all four kinds of atmospheric situations to

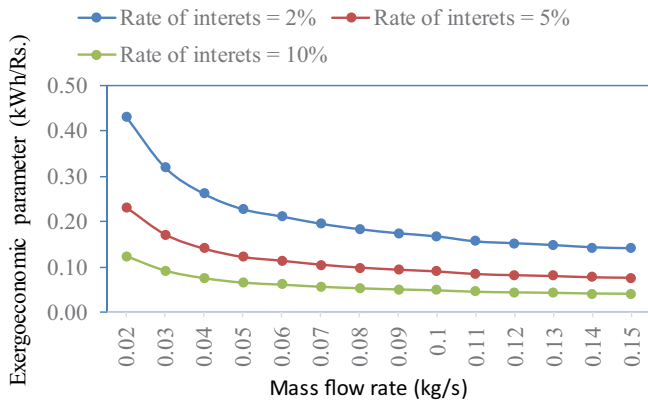


Fig. 8. Variation of exergoeconomic parameter with \dot{m}_f considering different rate of interest for UEOYAC for DS type SEOWP by incorporating N equal partially covered PVTCPs at $N = 4$.

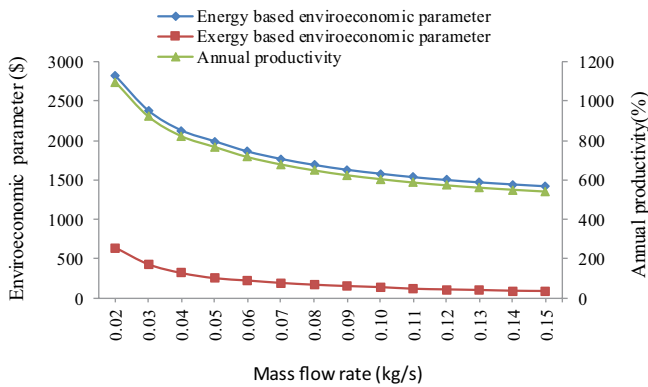


Fig. 9. Variation of enviroeconomic parameter and annual productivity with \dot{m}_f for DS type SEOWP by incorporating N equal partially covered PVTCPs at $N = 4$.

know the effect of \dot{m}_f on productivity, exergoeconomic and enviroeconomic parameters. Based on the current research study, the following conclusions have been made:

- The value of exergoeconomic parameter decreases with the increases in \dot{m}_f and it becomes almost constant after $\dot{m}_f = 0.11$ kg/s.
- The enviroeconomic parameter has been found to diminish with the increases in \dot{m}_f and it becomes almost constant after $\dot{m}_f = 0.12$ kg/s.
- The value of productivity has been found to be more than 100% corresponding to all values of \dot{m}_f which represent the feasibility of system for all values of \dot{m}_f . Further, productivity of NPVTCP- SEOWP-DS diminishes with the increase in the value of \dot{m}_f and it becomes almost constant after $\dot{m}_f = 0.11$ kg/s.

Symbols

A_{rm}	—	Area of receiver covered by PV module, m ²
A_{rc}	—	Area of receiver covered by glass, m ²
A_{am}	—	Area of aperture covered by PV module, m ²
A_{ac}	—	Area of aperture covered by glass, m ²

A_{gE}	—	Area of east glass cover, m ²
A_b	—	Area of basin, m ²
A_{gW}	—	Area of west glass cover, m ²
L	—	Latent heat, J/kg
L_g	—	Thickness of glass cover, m
K_g	—	Thermal conductivity of glass, W/m-K
$I_b(t)$	—	Beam radiation, W/m ²
T_a	—	Ambient temperature, °C
L_i	—	Thickness of insulation, m
K_i	—	Thermal conductivity of insulation, W/m-K
α_c	—	Absorptivity of the solar cell
\dot{m}_f	—	Mass flow rate of water, kg/s
τ_g	—	Transmissivity of the glass, fraction
C_p/C_w	—	Specific heat of water, J/kg-K
β_o	—	Temperature coefficient of efficiency, K ⁻¹
L_r	—	Total length of receiver area, m
L_a	—	Total length of aperture area, m
L_{rc}	—	Length of receiver covered by glass
L_{rm}	—	Length of receiver covered by PV module
L_{ac}	—	Length of aperture covered by glass
L_{am}	—	Length of aperture covered by PV module
η_c	—	Solar cell efficiency
η_m	—	PV module efficiency
η_{cN}	—	Temperature dependent electrical efficiency of solar cells of a number, (N) of PVT-CPC water collectors
b_r	—	Breath of receiver, m
b_o	—	Breath of aperture, m
$(\alpha\tau)_{eff}$	—	Product of effective absorptivity and transmittivity
F'	—	Collector efficiency factor
T_c	—	Solar cell temperature, °C
T_p	—	Absorber plate temperature, °C
L_p	—	Thickness of absorber plate, m
K_p	—	Thermal conductivity of absorber plate, W/m-K
T_{fi}	—	Fluid temperature at collector inlet, °C
T_f	—	Temperature of fluid in collector, °C
PF_1	—	Penalty factor due to the glass covers of module
PF_2	—	Penalty factor due to plate below the module
PF_3	—	Penalty factor due to the absorption plate for the glazed portion
PF_c	—	Penalty factor due to the glass covers for the glazed portion
β	—	Packing factor of the module
η_o	—	Efficiency at standard test condition
T_{ioN}	—	Outlet water temperature at the end of Nth PVT-CPC water collector, °C
h_i	—	Heat transfer coefficient for space between the glazing and absorption plate, W/m ² -K
h'_i	—	Heat transfer coefficient from bottom of PVT to ambient, W/m ² -K
h_o	—	Heat transfer coefficient from top of PVT to ambient, W/m ² -K
U_{tca}	—	Overall heat transfer coefficient from cell to ambient, W/m ² -K
U_{tcp}	—	Overall heat transfer coefficient from cell to plate, W/m ² -K

h_{pf}	—	Heat transfer coefficient from blackened plate to fluid, W/m ² -K
U_{tpa}	—	Overall heat transfer coefficient from plate to ambient, W/m ² -K
U_{Lm}	—	Overall heat transfer coefficient from module to ambient, W/m ² -K
U_{Lc}	—	Overall heat transfer coefficient from glassing to ambient, W/m ² -K
P_m	—	Annual power generated from photovoltaic module, kWh
P_u	—	Annual power utilized by pump, kWh
ϵ	—	Emissivity
α'	—	Absorptivity
\dot{E}_x	—	Hourly exergy, W
$I(t)$	—	Global solar intensity, W/m ²
$I_{SE}(t)$	—	Solar intensity on east glass cover, W/m ²
$I_{SW}(t)$	—	Solar intensity on west glass cover, W/m ²
T_{giE}	—	Glass temperature at inner surface of east glass cover, °C
T_{giW}	—	Glass temperature at inner surface of west glass cover, °C
h_{rwg}	—	Radiative heat transfer coefficient from water to inner surface of glass cover, W/m ² -K
h_{cwg}	—	Convective heat transfer coefficient from water to inner surface of glass cover, W/m ² -K
h_{ewgE}	—	Evaporative heat transfer coefficient for east side, W/m ² -K
h_{ewgW}	—	Evaporative heat transfer coefficient for west side, W/m ² -K
M_w	—	Mass of water in basin, kg
\dot{m}_{cw}	—	Mass of distillate from of double slope solar still, kg
M_{ew}	—	Annual yield from solar distillation system, kg
a	—	Clear days, blue sky
b	—	Hazy days, fully
c	—	Hazy and cloudy days, partially
d	—	Cloudy days, fully
\dot{Q}_{uN}	—	Rate of useful thermal output from N identical partially (25%) covered PVT-CPC water collectors connected in series, kWh
N	—	Life of PVT-CPC active solar distillation system, year
I	—	Rate of interest, %
$G_{ex,annual}$	—	Overall annual exergy gain, kWh
\ln	—	Natural logarithm
DS	—	Double slope
t	—	Time, h
R	—	Reflectivity
SEOWP	—	Solar energy operated water purifier
T_s	—	Temperature of sun, °C
T_w	—	Temperature of water in basin, °C
T_a	—	Ambient temperature, °C
T_{wo}	—	Water temperature at $t = 0$, °C
\bar{T}_{CN}	—	Average solar cell temperature
E_{out}	—	Overall annual energy available from PVT-CPC solar distillation system, kWh

Ex	—	Daily exergy, kWh
Exm	—	Monthly exergy, kWh
N	—	Number of PVT-CPC water collector
θ	—	Angle of inclination of glass cover with horizontal
NPVT-CPC	—	N equal partially covered PVT compound parabolic concentrating collectors
FPC	—	Flat plate collector
PVT	—	Photovoltaic thermal
CPC	—	Compound parabolic concentrator
N'	—	Number of sunshine hours
r'	—	Daily diffuse to daily global irradiation ratio

Subscripts

g	—	Glass
w	—	Water
E	—	East
W	—	West
in	—	Incoming
out	—	Outgoing
eff	—	Effective

References

- [1] S.N. Rai, G.N. Tiwari, Single basin solar still coupled with flat plate collector, *Energy Convers. Manage.*, 23 (1983) 145–149.
- [2] S. Kumar, A. Tiwari, An experimental study of hybrid photovoltaic thermal (PV/T) active solar still, *Int. J. Energy Res.*, 32 (2008) 847–858.
- [3] E.C. Kern, M.C. Russell, Combined Photovoltaic and Thermal Hybrid Collector Systems, Proceedings of the 13th IEEE Photovoltaic Specialists, June 5–8, Washington, DC, USA, pp. 1153–1157.
- [4] G. Singh, S. Kumar, G.N. Tiwari, Design, fabrication and performance of a hybrid photovoltaic/thermal (PVT) double slope active solar still, *Desalination*, 277 (2011) 399–406.
- [5] D.B. Singh, J.K. Yadav, V.K. Dwivedi, S. Kumar, G.N. Tiwari, I.M. Al-Helal, Experimental studies of active solar still integrated with two hybrid PVT collectors, *Sol. Energy*, 130 (2016) 207–223.
- [6] G.N. Tiwari, J.K. Yadav, D.B. Singh, I.M. Al-Helal, A.M. Abdel-Ghany, Exergoeconomic and enviroeconomic analyses of partially covered photovoltaic flat plate collector active solar distillation system, *Desalination*, 367 (2015) 186–196.
- [7] D.B. Singh, G.N. Tiwari, Enhancement in energy metrics of double slope solar still by incorporating N identical PVT collectors, *Sol. Energy*, 143 (2017) 142–161.
- [8] D.B. Singh, Exergoeconomic and enviroeconomic analyses of N identical photovoltaic thermal integrated double slope solar still, *Int. J. Exergy*, 23 (2017) 347–366.
- [9] D.B. Singh, N. Kumar, Harender, S. Kumar, S.K. Sharma, A. Mallick, Effect of depth of water on various efficiencies and productivity of N identical partially covered PVT collectors incorporated single slope solar distiller unit, *Desal. Water Treat.*, 138 (2019) 99–112.
- [10] D.B. Singh, Improving the performance of single slope solar still by including N identical PVT collectors, *Appl. Therm. Eng.*, 131 (2018) 167–179.
- [11] D.B. Singh, N. Kumar, S. Kumar, V.K. Dwivedi, J.K. Yadav, G.N. Tiwari, Enhancement in exergoeconomic and enviroeconomic parameters for single slope solar still by incorporating N identical partially covered photovoltaic collectors, *J. Sol. Energy Eng., Wind Energy Build. Energy Conserv.*, 140 (2018) 051002–1.

- [12] L. Sahota, G.N. Tiwari, Exergoeconomic and enviroeconomic analyses of hybrid double slope solar still loaded with nanofluids, *Energy Convers. Manage.*, 148 (2017) 413–430.
- [13] F. Carranza, C. Villa, J. Aguilera, H.A. Borbón-Nuñez, D. Saucedo, Experimental study on the potential of combining TiO_2 , ZnO , and Al_2O_3 nanoparticles to improve the performance of a double-slope solar still equipped with saline water preheating, *Desal. Water Treat.*, 216 (2021) 14–33.
- [14] M.R. Kouadri, N. Chennouf, M.H. Sellami, M.N. Raache, A. Benarima, The effective behavior of ZnO and CuO during the solar desalination of brackish water in southern Algeria, *Desal. Water Treat.*, 218 (2021) 126–134.
- [15] D. Atheaya, A. Tiwari, G.N. Tiwari, I.M. Al-Helal, Analytical characteristic equation for partially covered photovoltaic thermal (PVT) – compound parabolic concentrator (CPC), *Sol. Energy*, 111 (2015) 176–85.
- [16] R. Tripathi, G.N. Tiwari, I.M. Al-Helal, Thermal modelling of N partially covered photovoltaic thermal (PVT)–Compound parabolic concentrator (CPC) collectors connected in series, *Sol. Energy*, 123 (2016) 174–84.
- [17] D.B. Singh, G.N. Tiwari, Performance analysis of basin type solar stills integrated with N identical photovoltaic thermal (PVT) compound parabolic concentrator (CPC) collectors: a comparative study, *Sol. Energy*, 142 (2017) 144–158.
- [18] D.B. Singh, G.N. Tiwari, Exergoeconomic, enviroeconomic and productivity analyses of basin type solar stills by incorporating N identical PVT compound parabolic concentrator collectors: a comparative study, *Energy Convers. Manage.*, 135 (2017) 129–147.
- [19] D.B. Singh, G.N. Tiwari, Effect of energy matrices on life cycle cost analysis of partially covered photovoltaic compound parabolic concentrator collector active solar distillation system, *Desalination*, 397 (2016) 75–91.
- [20] V.S. Gupta, D.B. Singh, R.K. Mishra, S.K. Sharma, G.N. Tiwari, Development of characteristic equations for PVT-CPC active solar distillation system, *Desalination*, 445 (2018) 266–279.
- [21] V.S. Gupta, D.B. Singh, S.K. Sharma, N. Kumar, T.S. Bhatti, G.N. Tiwari, Modeling self-sustainable fully-covered photovoltaic thermal-compound parabolic concentrators connected to double slope solar distiller, *Desal. Water Treat.*, 190 (2020) 12–27.
- [22] V. Singh, D.B. Singh, N. Kumar, R. Kumar, Effect of number of collectors (N) on life cycle conversion efficiency of single slope solar desalination unit coupled with N identical partly covered compound parabolic concentrator collectors, *Mater. Today: Proc.*, 28 (2020) 2185–2189.
- [23] D.B. Singh, G. Singh, N. Kumar, P.K. Singh, R. Kumar, Effect of mass flow rate on energy payback time of single slope solar desalination unit coupled with N identical compound parabolic concentrator collectors, *Mater. Today: Proc.*, 28 (2020) 2551–2556.
- [24] G.K. Sharma, N. Kumar, D.B. Singh, A. Mallick, Exergoeconomic analysis of single slope solar desalination unit coupled with PVT-CPCs by incorporating the effect of dissimilarity of the rate of flowing fluid mass, *Mater. Today: Proc.*, 28 (2020) 2364–2368.
- [25] H. Prasad, P. Kumar, R.K. Yadav, A. Mallick, N. Kumar, D.B. Singh, Sensitivity analysis of N identical partially covered (50%) PVT compound parabolic concentrator collectors integrated double slope solar distiller unit, *Desal. Water Treat.*, 153 (2019) 54–64.
- [26] K. Bharti, S. Manwal, C. Kishore, R.K. Yadav, P. Tiwar, D.B. Singh, Sensitivity analysis of n alike partly covered PVT flat plate collectors integrated double slope solar distiller unit, *Desal. Water Treat.*, 211 (2021) 45–59.
- [27] D.B. Singh, Sensitivity analysis of N identical evacuated tubular collectors integrated double slope solar distiller unit by incorporating the effect of exergy, *Int. J. Exergy*, 34 (2021) 424–447.
- [28] K. Sampathkumar, T.V. Arjunan, P. Senthilkumar, The experimental investigation of a solar still coupled with an evacuated tube collector, *Energy Sources Part A*, 35 (2013) 261–270.
- [29] R.V. Singh, S. Kumar, M.M. Hasan, M.E. Khan, G.N. Tiwari, Performance of a solar still integrated with evacuated tube collector in natural mode, *Desalination*, 318 (2013) 25–33.
- [30] S. Kumar, A. Dubey, G.N. Tiwari, A solar still augmented with an evacuated tube collector in forced mode, *Desalination*, 347 (2014) 15–24.
- [31] R.K. Mishra, V. Garg, G.N. Tiwari, Thermal modeling and development of characteristic equations of evacuated tubular collector (ETC), *Sol. Energy*, 116 (2015) 165–176.
- [32] D.B. Singh, V.K. Dwivedi, G.N. Tiwari, N. Kumar, Analytical characteristic equation of N identical evacuated tubular collectors integrated single slope solar still, *Desal. Water Treat.*, 88 (2017) 41–51.
- [33] D.B. Singh, G.N. Tiwari, Analytical characteristic equation of N identical evacuated tubular collectors integrated double slope solar still, *J. Sol. Energy Eng., Wind Energy Build. Energy Conserv.*, 135 (2017) 051003(1–11).
- [34] D.B. Singh, G.N. Tiwari, Energy, exergy and cost analyses of N identical evacuated tubular collectors integrated basin type solar stills: a comparative study, *Sol. Energy*, 155 (2017) 829–846.
- [35] R.J. Issa, B. Chang, Performance study on evacuated tubular collector coupled solar Still in west Texas climate, *Int. J. Green Energy*, 14 (2017) 793–800.
- [36] D.B. Singh, I.M. Al-Helal, Energy metrics analysis of N identical evacuated tubular collectors integrated double slope solar still, *Desalination*, 432 (2018) 10–22.
- [37] D.B. Singh, N. Kumar, A. Raturi, G. Bansal, A. Nirala, N. Sengar, Effect of Flow of Fluid Mass Per Unit Time on Life Cycle Conversion Efficiency of Double Slope Solar Desalination Unit Coupled with N Identical Evacuated Tubular Collectors, *Lecture Notes in Mechanical Engineering, Advances in Manufacturing and Industrial Engineering, Select Proceedings of ICAPIE 2019*, 2021, pp. 393–402.
- [38] S.K. Sharma, D.B. Singh, A. Mallick, S.K. Gupta, Energy metrics and efficiency analyses of double slope solar distiller unit augmented with N identical parabolic concentrator integrated evacuated tubular collectors: a comparative study, *Desal. Water Treat.*, 195 (2020) 40–56.
- [39] S.K. Sharma, A. Mallick, S.K. Gupta, N. Kumar, D.B. Singh, G.N. Tiwari, Characteristic equation development for double slope solar distiller unit augmented with N identical parabolic concentrator integrated evacuated tubular collectors, *Desal. Water Treat.*, 187 (2020) 178–194.
- [40] R.V. Patel, K. Bharti, G. Singh, R. Kumar, S. Chhabra, D.B. Singh, Solar still performance investigation by incorporating the shape of basin liner: a short review, *Mater. Today: Proc.*, 43 (2021) 597–604.
- [41] R.V. Patel, K. Bharti, G. Singh, G. Mittal, D.B. Singh, A. Yadav, Comparative investigation of double slope solar still by incorporating different types of collectors: a mini review, *Mater. Today: Proc.*, 38 (2021) 300–304.
- [42] R.V. Patel, G. Singh, K. Bharti, R. Kumar, D.B. Singh, A mini review on single slope solar desalination unit augmented with different types of collectors, *Mater. Today: Proc.*, 38 (2021) 204–210.
- [43] G. Singh, D.B. Singh, S. Kumara, K. Bharti, S. Chhabra, A review of inclusion of nanofluids on the attainment of different types of solar collectors, *Mater. Today: Proc.*, 38 (2021) 153–159.
- [44] G. Bansal, D.B. Singh, C. Kishore, V. Dogra, Effect of absorbing material on the performance of solar still: a mini review, *Mater. Today: Proc.*, 26 (2020) 1884–1887.
- [45] P. Shankar, A. Dubey, S. Kumar, G.N. Tiwari, Production of clean water using ETC integrated solar stills: thermoenviroeconomic assessment, *Desal. Water Treat.*, 218 (2021) 106–118.
- [46] S. Abdallah, M. Nasir, D. Afaneh, Performance evaluation of spherical and pyramid solar stills with chamber stepwise basin, *Desal. Water Treat.*, 218 (2021) 119–125.
- [47] D.L. Evan, Simplified method for predicting PV array output, *Sol. Energy*, 27 (1981) 555–560.
- [48] T. Schott, Operational Temperatures of PV Modules, *Proceedings of 6th PV Solar Energy Conference*, 1985, pp. 392–396.
- [49] B.J. Huang, T.H. Lin, W.C. Hung, F.S. Sun, Performance evaluation of solar photovoltaic/thermal systems, *Sol. Energy*, 70 (2001) 443–448.
- [50] P.K. Nag, *Basic and Applied Thermodynamics*, Tata McGraw-Hill, ISBN 0-07-047338-2, 2004.

- [51] P.I. Cooper, Digital simulation of experimental solar still data, *Sol. Energy*, 14 (1973) 451.
- [52] R.V. Dunkle, Solar Water Distillation, the Roof Type Solar Still and Multi Effect Diffusion Still, *International Developments in Heat Transfer*, A.S.M.E., Proceedings of international Heat transfer, Part V(1961) 895, University of Colorado.
- [53] G.N. Tiwari, R.K. Mishra, *Advanced Renewable Energy Sources*, Royal Society of Chemistry Publishing House, UK, ISBN 978-1-84973-380-9, 2012.
- [54] H. Ashcroft, The productivity of several machines under the care of one operator, *J. R. Stat. Soc. (Lond.) Ser. B XII*, 12 (1950) 145–151.
- [55] F. Benson, Further notes on the productivity of machines requiring attention at random intervals, *J. R. Stat. Soc. Ser. B XIV*, 14 (1952) 200–210.
- [56] D.R. Cox, The productivity of machines requiring attention at random intervals, *J. R. Stat. Soc. Ser. B XIII*, 13 (1951) 65–82.
- [57] International Labor Office, *Introduction to Work Study*, International Labor Organization, Geneva, ISBN 81-204-0602-8, 1979.
- [58] B.Y.H. Liu, R.C. Jordan, The interrelationship and characteristic distribution of direct, diffuse and total solar radiation, *Sol. Energy*, 4 (1960) 1–19.

Appendix-A

Expressions for various terms used in Eqs. (1) and (2) are as follows.

$$U_{\text{tca}} = \left[\frac{1}{h_o} + \frac{L_g}{K_g} \right]^{-1}; U_{\text{tcp}} = \left[\frac{1}{h_i} + \frac{L_g}{K_g} \right]^{-1};$$

$$h_o = 5.7 + 3.8V, \text{ Wm}^{-2}\text{K}^{-1}; h_i = 5.7, \text{ Wm}^{-2}\text{K}^{-1};$$

$$U_{\text{tpa}} = \left[\frac{1}{U_{\text{tca}}} + \frac{1}{U_{\text{tcp}}} \right]^{-1} + \left[\frac{1}{h'_i} + \frac{1}{h_{\text{pf}}} + \frac{L_i}{K_i} \right]^{-1}; h_{\text{pf}} = 100 \text{ Wm}^{-2}\text{K}^{-1}$$

$$h'_i = 2.8 + 3V', \text{ Wm}^{-2}\text{K}^{-1};$$

$$U_{L1} = \frac{U_{\text{tcp}} U_{\text{tca}}}{U_{\text{tcp}} + U_{\text{tca}}}; U_{L2} = U_{L1} + U_{\text{tpa}};$$

$$U_{Lm} = \frac{h_{\text{pf}} U_{L2}}{F' h_{\text{pf}} + U_{L2}}; U_{Lc} = \frac{h_{\text{pf}} U_{\text{tpa}}}{F' h_{\text{pf}} + U_{\text{tpa}}};$$

$$PF_1 = \frac{U_{\text{tcp}}}{U_{\text{tcp}} + U_{\text{tca}}}; PF_2 = \frac{h_{\text{pf}}}{F' h_{\text{pf}} + U_{L2}}; PF_c = \frac{h_{\text{pf}}}{F' h_{\text{pf}} + U_{\text{tpa}}};$$

$$(\alpha\tau)_{\text{leff}} = \rho(\alpha_c - \eta_c) \tau_g \beta_c \frac{A_{\text{am}}}{A_{\text{rm}}}; (\alpha\tau)_{\text{2eff}} = \rho \alpha_p \tau_g^2 (1 - \beta_c) \frac{A_{\text{am}}}{A_{\text{rm}}};$$

$$(\alpha\tau)_{\text{meff}} = [(\alpha\tau)_{\text{leff}} + PF_1 (\alpha\tau)_{\text{2eff}}]; (\alpha\tau)_{\text{ceff}} = PF_c \cdot \rho \alpha_p \tau_g \frac{A_{\text{ac}}}{A_{\text{rc}}};$$

$$A_{\text{rm}} = b_r L_{\text{rm}}; A_{\text{am}} = b_o L_{\text{am}};$$

$$A_c F_{\text{Rc}} = \frac{\dot{m}_f c_f}{U_{Lc}} \left[1 - \exp\left(\frac{-F' U_{Lc} A_c}{\dot{m}_f c_f}\right) \right];$$

$$A_m F_{\text{Rm}} = \frac{\dot{m}_f c_f}{U_{Lm}} \left[1 - \exp\left(\frac{-F' U_{Lm} A_m}{\dot{m}_f c_f}\right) \right];$$

$$(AF_R(\alpha\tau))_1 = \left[A_c F_{\text{Rc}}(\alpha\tau)_{\text{ceff}} + PF_2(\alpha\tau)_{\text{meff}} A_m F_{\text{Rm}} \left(1 - \frac{A_c F_{\text{Rc}} U_{Lc}}{\dot{m}_f c_f} \right) \right];$$

$$(AF_R U_L)_1 = \left[A_c F_{\text{Rc}} U_{Lc} + A_m F_{\text{Rm}} U_{Lm} + A_m F_{\text{Rm}} U_{Lm} \left(1 - \frac{A_c F_{\text{Rc}} U_{Lc}}{\dot{m}_f c_f} \right) \right]$$

$$K_K = \left(1 - \frac{(AF_R U_L)_1}{\dot{m}_f c_f} \right)$$

$$(AF_R(\alpha\tau))_{m1} = PF_2(\alpha\tau)_{\text{meff}} A_m F_{\text{Rm}}$$

$$(AF_R U_L)_{m1} = A_m F_{\text{Rm}} U_{Lm}$$

$$K_m = \left(1 - \frac{A_m F_{\text{Rm}} U_{Lm}}{\dot{m}_f c_f} \right)$$

Expressions for various terms used in Eqs. (4)–(15) are as follows.

$$a = \frac{1}{M_w C_w} \left[\frac{\dot{m}_f c_f (1 - K_k^N) + U_b A_b + h_{1wE} (P - A_2) A_b + h_{1wW} (P - B_2) A_b}{2P} \right];$$

$$\bar{f}(t) = \frac{1}{M_w C_w} \left[\left(\frac{\alpha'_w}{2} + h_1 \alpha'_b \right) A_b (\bar{I}_{SE}(t) + \bar{I}_{SW}(t)) + \frac{(1 - K_k^N)}{(1 - K_k)} (AF_R(\alpha\tau))_1 \bar{I}_b(t) + \left(\frac{(1 - K_k^N)}{(1 - K_k)} (AF_R U_L)_1 + U_b A_b \right) T_a + \left(\frac{h_{1wE} A_1 + h_{1wW} B_1}{P} \right) \frac{A_b}{2} \right];$$

$$A_1 = R_1 U_1 A_{gE} + R_2 h_{EW} A_{gW}$$

$$A_2 = h_{1wE} U_2 \frac{A_b}{2} + h_{EW} h_{1wW} \frac{A_b}{2}$$

$$P = \left(U_1 U_2 - \frac{h_{EW}^2 h_{1wW}}{A_{gE}} \frac{A_b}{2} \right) A_{gW}$$

$$U_1 = \frac{h_{1wE} \frac{A_b}{2} + h_{EW} A_{gE} + U_{c,gaE} A_{gE}}{A_{gW}}$$

$$U_2 = \frac{h_{1wW} \frac{A_b}{2} + h_{EW} A_{gW} + U_{c,gaW} A_{gW}}{A_{gE}}$$

$$B_1 = \frac{(R_2 P + A_1 h_{EW}) A_{gW}}{U_2 A_{gE}}$$

$$B_2 = \frac{P h_{1wW} \frac{A_b}{2} + h_{EW} A_{gW} A_2}{U_2 A_{gE}}$$

$$R_1 = \alpha'_s I_{SE}(t) + U_{c,gAE} T_a$$

$$R_2 = \alpha'_s I_{SW}(t) + U_{c,gAW} T_a$$

$$h_{EW} = 0.034 \times 5.67 \times 10^{-8} \left[(T_{giE} + 273)^2 + (T_{giW} + 273)^2 \right] \left[T_{giE} + T_{giW} + 546 \right]$$

$$U_{c,gAE} = \frac{\frac{K_g}{l_g} h_{1gE}}{\frac{K_g}{l_g} + h_{1gE}}; U_{c,gAW} = \frac{\frac{K_g}{l_g} h_{1gW}}{\frac{K_g}{l_g} + h_{1gW}}$$

$$h_{1gE} = 5.7 + 3.8V; h_{1gW} = 5.7 + 3.8V;$$

$$h_{1wE} = h_{rwgE} + h_{cwgE} + h_{ewgE}$$

$$h_{1wW} = h_{rwgW} + h_{cwgW} + h_{ewgW}$$

$$h_{e,wgE} = 16.273 \times 10^{-3} h_{c,wgE} \left[\frac{P_w - P_{giE}}{T_w - T_{giE}} \right];$$

$$h_{c,wgE} = 0.884 \left[(T_w - T_{giE}) + \frac{(P_w - P_{giE})(T_w + 273)}{268.9 \times 10^3 = P_w} \right]^{1/3};$$

$$h_{c,wgW} = 0.884 \left[(T_w - T_{giW}) + \frac{(P_w - P_{giW})(T_w + 273)}{268.9 \times 10^3 = P_w} \right]^{1/3};$$

$$P_w = \exp \left[25.317 - \frac{5144}{T_w + 273} \right];$$

$$P_{giE} = \exp \left[25.317 - \frac{5144}{T_{giE} + 273} \right];$$

$$P_{giW} = \exp \left[25.317 - \frac{5144}{T_{giW} + 273} \right];$$

$$h_{rwgE} = (0.82 \times 5.67 \times 10^{-8}) \left[(T_w + 273)^2 + (T_{giE} + 273)^2 + (T_{giE} + 273)^2 \right] \left[T_w + T_{giE} + 546 \right];$$

$$h_{rwgW} = (0.82 \times 5.67 \times 10^{-8}) \left[(T_w + 273)^2 + (T_{giW} + 273)^2 + (T_{giW} + 273)^2 \right] \left[T_w + T_{giW} + 546 \right];$$